LBL-33341
UC-410

Lawrence Berkeley Laboratory
UNIVERSITY OF CALIFORNIA

Accelerator & Fusion
Research Division

Presented at the SPIE 1993 International Symposium on
Optical Applied Science and Engineering, San Diego, CA,
July 11–16, 1993, and to be published in the Proceedings

Analysis of Insertion Device Magnet Measurements for the Advanced Light Source

S. Marks, D. Humphries, B. Kincaid, R. Schlueter, and C. Wang

July 1993

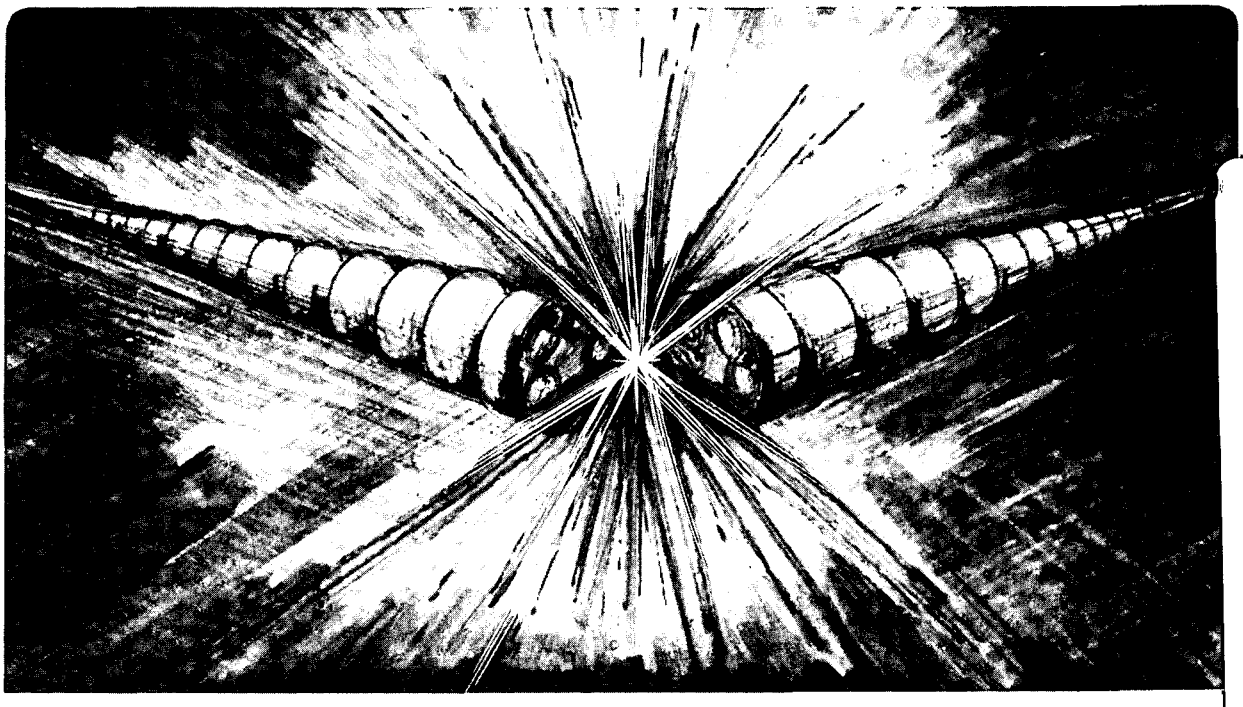

Prepared for the U.S. Department of Energy under Contract Number DE-AC03-76SF00098

DISCLAIMER

LBL-33341

Analysis of Insertion Device Magnet Measurements for the Advanced Light Source*

S. Marks, D. Humphries, B. Kincaid, R. Schlueter, and C. Wang

Advanced Light Source
Accelerator and Fusion Research Division
Lawrence Berkeley Laboratory
University of California
Berkeley, CA 94720

July 1993

Paper Presented at the SPIE 1993 International Symposium on Optical Applied Science and Engineering
San Diego, CA
July 11-16, 1993

*This work was supported by the Director, Office of Energy Research, Office of Basic Energy Sciences, Materials Sciences Division of the U.S. Department of Energy, under Contract No. DE-AC03-76SF00098.

Analysis of insertion device magnet measurements for the Advanced Light Source

S. Marks, D. Humphries, B. M. Kincaid, R. Schlueter, C. Wang

Lawrence Berkeley Laboratory, University of California
1 Cyclotron Road, Berkeley, California 94720

ABSTRACT

The Advanced Light Source (ALS) , which is currently being commissioned at Lawrence Berkeley Laboratory, is a third generation light source designed to produce XUV radiation of unprecedented brightness. To meet the high brightness goal the storage ring has been designed for very small electron beam emittance and the undulators installed in the ALS are built to a high degree of precision. The allowable magnetic field errors are driven by electron beam and radiation requirements. Detailed magnetic measurements and adjustments are performed on each undulator to qualify it for installation in the ALS. The first two ALS undulators, IDA and IDB, have been installed.

This paper describes the program of measurements, data analysis, and adjustments carried out for these two devices. Calculations of the radiation spectrum, based upon magnetic measurements, are included. Final field integral distributions are also shown. Good field integral uniformity has been achieved using a novel correction scheme, which is also described.

1. INTRODUCTION

The first two insertion devices, IDA and IDB, which are both 5.0 cm period undulators, have been measured, qualified and installed in the ALS. Construction is complete for a third device, an 8.0 cm period undulator, however, magnetic measurements have not yet been carried out. ALS undulators are of the Halbach hybrid permanent magnet type.[1] The basic structure consists of permanent magnet blocks sandwiched between soft iron poles. For ALS devices, the permanent magnet material is Nd-Fe-B and the poles are made of vanadium permendur. Figure 1 illustrates the top portion of one-half period of the structure.

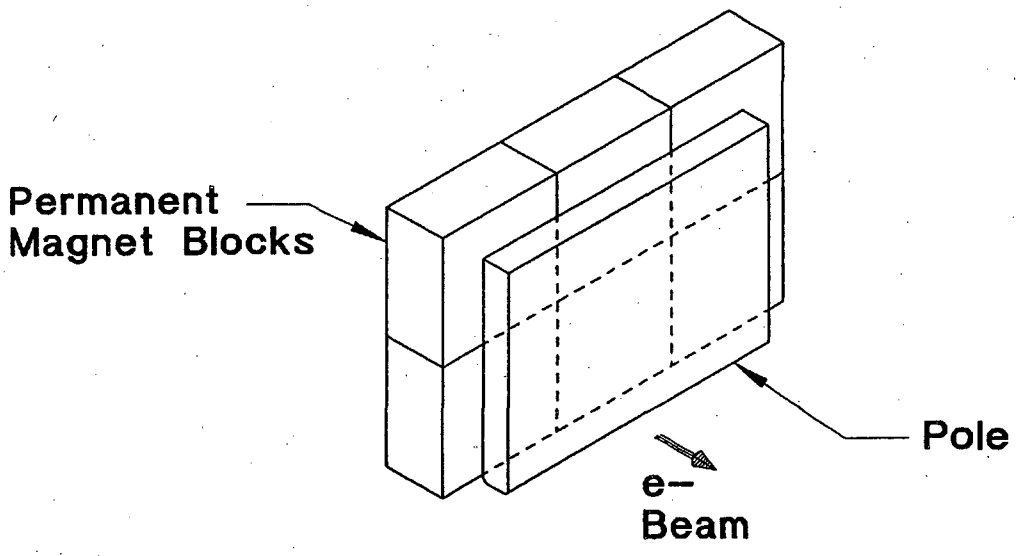

Figure 1. Hybrid pole structure.

The hybrid design produces higher peak fields compared to a pure permanent magnet device. Of equal importance, field errors are easier to control, since the primary influence is the dimension and placement of the poles. However for the tight error tolerances required of ALS undulators, magnetic field errors resulting from the direct fields from the permanent magnet blocks can also be significant.

Magnetic field errors can be divided into those that degrade the spectral brightness of the emitted radiation, and those that have a deleterious effect on the electron beam. The second category includes influences on both the main electron beam as well as scattered particles. Deterioration of the radiation spectrum results from the loss of phase coherence associated with deviations from the ideal periodic electron trajectory. Trajectory deviations may be the result of either a distribution of local field perturbations or long-range, systematic field errors, such as an integrated dipole or the systematic peak field variation due to a gap taper.

Electron dynamics is primarily influenced by the total field line integral through a device, since an undulator is typically small compared to a betatron wavelength. Of particular significance is the lack of uniformity in line integrals for different electron paths through a device. Consider field line integral, where lines of integration are parallel to the axis and are defined by the radial displacement from the axis, r. The distribution of integral values as a function of r can be expanded as a Taylor series. The Taylor series is equivalent to a multipole expansion representation of the integrated magnetic field within the magnetic aperture, defined by the undulator gap. The main electron beam generally stays well within the central magnetic aperture. Therefore, the influence on beam dynamics, such as a tune shift, can be evaluated in terms of the multipole coefficients. The magnetic aperture corresponds to the radius of convergence for the Taylor series, and, therefore, integrated errors outside this radius are not predictable by the multipole coefficients. Electrons may be scattered outside the magnetic aperture by gas collisions or intra-bunch collisions. The trajectories of scattered electrons whose maximum excursion from the central axis is within an envelope, called the dynamic aperture, will damp back down to the main beam envelope. Electrons outside the dynamic aperture are lost, and the electron beam lifetime is decreased. Magnetic field errors outside the magnetic aperture can affect the dynamic aperture.

In general, after a device has been characterized magnetically, adjustments of features of an undulator's magnetic field may be required. In principle, these adjustments may include alteration of line integrals to reduce damaging affects on the electron beam as well as fine tuning of local field errors to improve spectral performance. The design of the magnetic structure for the ALS undulators places an emphasis on mechanical precision of the periodic structure rather than ease of adjustment of local field perturbations.[2] This strategy has proven successful; no adjustments of this type were required for the first devices. However, mechanisms are incorporated in the design of the end structure to adjust field integrals. A permanent magnet rotor mechanism in the ends provides a means for adjusting the integrated dipole of the device.[3] An additional magnetic structure installed in the ends of the device incorporates an array of permanent magnets to alter the field integral distribution relative to the integral value along the axis. This mechanism is described in the final section of this paper.

A custom magnetic measurement facility was designed and built for qualification of ALS insertion devices. The primary features include a stage designed to translate through the gap. Hall probes are mounted to the stage to measure both the vertical field, B_y, and the horizontal field, B_x. Probe position within the gap can be varied by movement of the stage. Precision position monitoring is maintained with the use of a laser interferometer system. The magnetic measurement facility is described in more detail elsewhere.[4]

In addition to the Hall probe system, an integral coil is also used to measure total field integrals, $\int B_y \cdot dz$ and $\int B_x \cdot dz$. The assembly consists of a 100 turn coil wound onto a G10 (epoxy fiberglass) mandrel which is installed into a G10 support in one of two possible orientations. One orientation is for measuring $\int B_y \cdot dz$, and the other is for measuring $\int B_x \cdot dz$. The coil is 5.5 m long (ALS undulators are 4.5 m long). The coil width is 1 cm. The coil sensitivity is 1×10^{-6} V-sec = 1 G-cm. The integral coil provides the primary measurement of $\int B_x \cdot dz$, since a strong nonlinear coupling to the B_y component affects Hall probe measurements of B_x. This effect is generally called the planar Hall effect. A method for extracting reliable B_x values from Hall probe data is currently under investigation.

A typical Hall probe scan consists of 2500 samples spaced at an average interval of 2.2 mm along the axis. Scans are taken at multiple gaps between the minimum operating gap of 14 mm and the maximum gap of 210 mm. At each gap, scans are taken at the axial center and at several horizontal and vertical offsets from the center.

2. DATA ANALYSIS TOOLS

Magnetic field data is reduced and analyzed using a set of analytical tools developed for this purpose. Initial data reduction converts interferometer counts and Hall probe voltage for each sample into a file of axial position and magnetic field pairs. The next level of processing performs a spline fit to the data, including first and second integrals and first and second derivatives. Special analytical tools have been developed for a variety of higher level processing options. These include identification of field peaks, truncation to eliminate end fields, a nonlinear least-squares harmonic fit, Fourier transform of the field, a half-period filter transform of the field, and optical phase and radiation spectrum calculations. The harmonic fit and half-period filter are described in more detail below.

Figure 2 shows the spline fit to a field scan of B_y. Data is shown for one half of the device, for z = -2500 mm to 0 mm. Note that the origin of the coordinate system is set at the middle of the device, i.e., the center of the center pole. The field is nominally symmetric about z = 0. Only one half of the data, corresponding to z < 0, is shown in Figure 2, so that details of the graph can be seen with greater clarity. Notice that the field deviates from periodicity at the ends, where a transition occurs from a periodic field in the middle to zero field outside the device. For analysis of the periodic portion of the field, it is truncated to include, for example, the portion between z = ±2000 mm. The truncated periodic data is relevant for evaluation of spectral performance. In particular, deviations from ideal periodicity are evaluated.

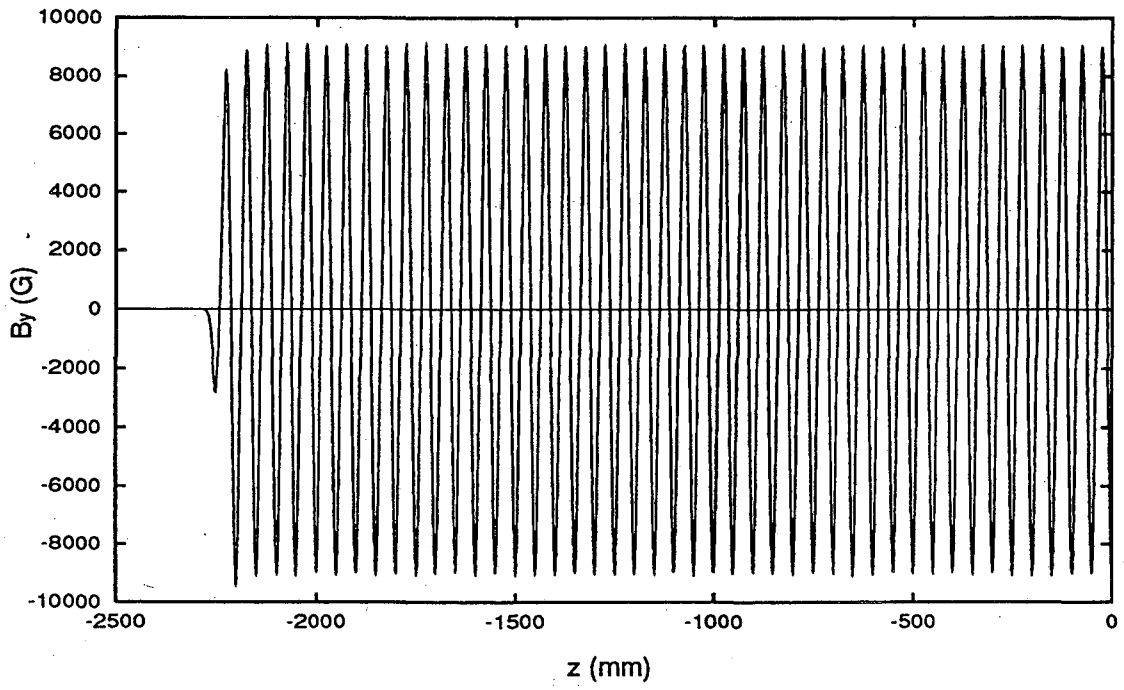

Figure 2. Spline fit for Hall probe scan of B_y. Data corresponds to axial scan of IDA at minimum gap of 14 mm.

A harmonic fit is performed on a truncated data set, excluding the end fields. The data is fit to a function of the form of equation (1).

$$B_h(z) = \sum_n a_n \cos(nkz + \phi_n);\ n = 1, 3, 5, \ldots \quad (1)$$

A nonlinear least squares fit routine is used, where the adjustable parameters are the coefficients a_n, the phase terms ϕ_n, and $k = 2\pi/\lambda_u$, where λ_u is the undulator period. The harmonic residual is defined as the difference between the measured values, $B_y(z)$, and the fit function values, $B_h(z)$, as defined in equation (2).

$$R_h(z) = B_y(z) - B_h(z) \tag{2}$$

The rms value of the residual over the full length of the fit is a measure of the total distribution of field errors. Note that since the harmonic fit is calculated over the full length of the periodic portion of the field, the harmonic residual includes both local field errors and long range errors, such as gap taper.

The half period filter function defined by equation (3) provides an alternate measure of field errors.

$$\begin{aligned} F_h(z) &= \frac{1}{2}B(z+\lambda_u/4) + B(z-\lambda_u/4) \\ &= \frac{1}{2}\int B(\xi)[\delta(\xi - z - \lambda_u/4) + \delta(\xi - z + \lambda_u/4)]d\xi \\ &= \mathcal{F}^{-1}\{\mathcal{F}[B(\xi)]\cdot\mathcal{F}[\delta(\xi - z - \lambda_u/4) + \delta(\xi - z + \lambda_u/4)]\} \end{aligned} \tag{3}$$

Notice that the value of this function is zero throughout the periodic portion of a perfect device; all odd harmonics of a periodic field cancel. The second form of equation (3) is an equivalent convolution integral. The third form of the equation shows the Fourier transform method of calculating a convolution; this is the method that is actually used to calculate the half-period filter. The half-period filter provides a measure of field errors over a one half-period range; i.e., this provides some measure of local field errors. Figure 3 shows the half-period filter transform of the field graphed in Figure 2. Notice that the function has small values within the periodic region of the field, for z > -2000. An rms value for the function in this region provides some measure of the total level of local field deviations. The function values in the end region are very large in comparison. This does not represent an error per se; rather, it is a generic function of the transition from the periodic field inside the undulator to zero field outside the device.

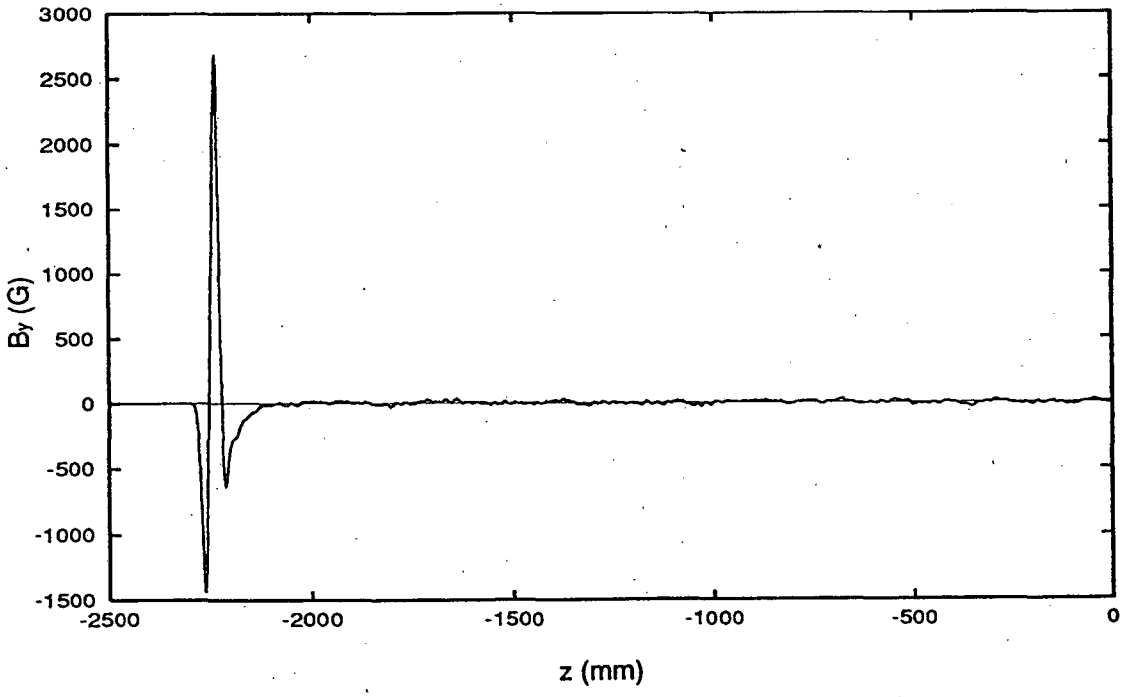

Figure 3. Half-period filter output for Hall probe scan of B_y.

The half-period filter provides a dramatic delineation of the periodic portion of the field from the ends. This carries over to integral values as well. From an examination of equation (3), it is clear that the integral of the half-period filter function is equivalent to the integral of $B(z)$, as long as the limits of integration correspond to constant field regions. In

particular, since the value of the function is small everywhere except at the ends, integration of the half-period filter provides an accurate mechanism for separating out the contributions to the total integral from the ends and from the periodic middle portion of the field. This separation of integral components is essential in the magnetic adjustment process. It allows for the characterization of the magnetic excitation of the end rotors used to adjust the integrated dipole. It also allows for the characterization of integrated field error distributions in the periodic structure, so that the permanent magnet array incorporated in the end structure can be adjusted to offset the errors. Integrals of the half-period function are also rich in qualitative information since a local value corresponds to the average integral of the field, stripped of the periodic oscillations. The first integral corresponds to the average transverse particle velocity, and the second integral corresponds to the average particle trajectory.

3. RADIATION SPECTRUM

The U5.0 undulators, IDA and IDB, are designed to operate over the spectral range from 50 eV to 1900 eV. The low energy limit of the range requires that B_{eff} is 0.833 T at the minimum gap. B_{eff} is defined in equation (4) below.

$$B_{eff}^2 = \sum_n \frac{1}{n^2} a_n^2 \; ; \; n = 1, 3, 5, \ldots \tag{4}$$

The coefficients a_n are the harmonic coefficients for the magnetic field. A measured value for B_{eff} of 0.846 T is achieved at the minimum gap of 14 mm for IDA and IDB. To reach the high energy portion of the range, high brightness must be produced in the 3rd and 5th harmonic of the spectrum. The brightness is degraded by random magnetic field errors. This effect increases for higher harmonics. Kincaid developed a theoretical model of the degradation of undulator radiation from random errors,[5] which shows that peak flux density is degraded by a factor e^{-30q}, where q is defined by equation (5).

$$q = n^2 \sigma^2 N \left[\frac{K^2/2}{1 + K^2/2} \right]^2 \tag{5}$$

The factor σ is the rms random field error, n is harmonic number, N is the number of undulator periods, and K is the deflection parameter defined by equation (6).

$$K = \frac{eB_0 \lambda_u}{2\pi mc} = 0.934 B_0(T) \lambda_u(cm) \tag{6}$$

Here e is the electron charge, m is the electron mass, c is the speed of light, B_0 is the peak field, and λ_u is the undulator period length. A goal of achieving 70% the ideal flux density for the fifth harmonic was established for ALS undulators. The ideal value corresponds to an ideal periodic field of the same B_{eff}. Using Kincaid's criterion to estimate the degradation at the minimum gap, the rms value of random errors must be less than 0.25%.

The maximum tolerable random error value of 0.25% was used as a basis for establishing mechanical tolerances.[6] This number is also used as a benchmark to assess measured magnetic fields. However, deriving a measure of random field errors from magnetic data is not straightforward. The harmonic residual and half-period filter, described in section 2, may be considered for this purpose. Remember that the rms value of the harmonic residual includes the effects of both random and systematic errors. The rms value of the half-period filter measures short-range errors and is therefore probably a more accurate indicator of random errors. Typical rms values, normalized by B_{eff}, for measured fields of IDA and IDB at the minimum gap of 14 mm are 0.24% and 0.18% for the harmonic residual and half-period filter, respectively. The final assessment of spectral performance of ALS undulators is based upon the direct calculation of spectral properties using measured field data as input. The calculations use a program called *RADID* that is based upon an algorithm developed by Wang.[7]

Figure 4 shows the calculated single electron radiation spectrum corresponding to a data scan on the central axis at a gap of 14 mm and a current of 400 mA, which is the design current for the ALS storage ring. The 5th harmonic for this spectrum is 72% of the ideal spectrum. Figure 5 shows the ratio of the real to ideal 5th harmonic flux density as a function of K_{eff}, where this is defined from equation (6) using B_{eff} as the peak value. A K_{eff} value of 3.94 corresponds to the minimum gap of 14 mm, and a value of 0.45 corresponds to a 47 mm gap.

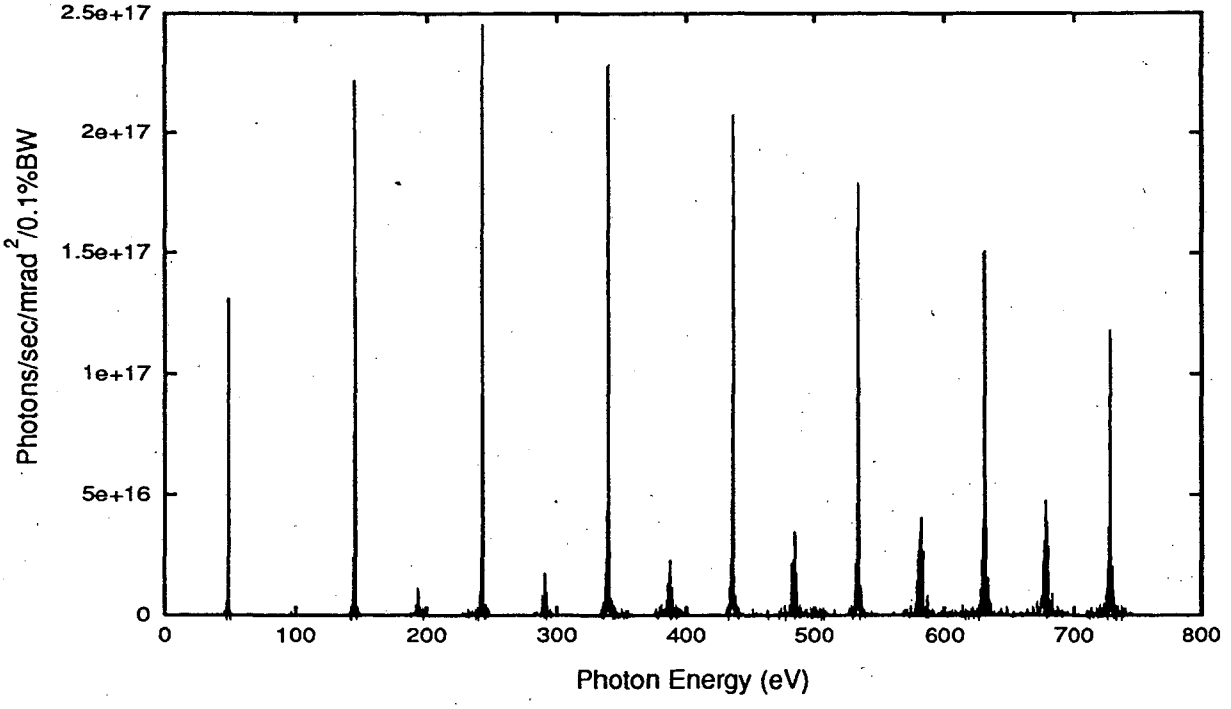

Figure 4. Calculated single electron flux density for IDB at 14 mm gap and 400 mA current.

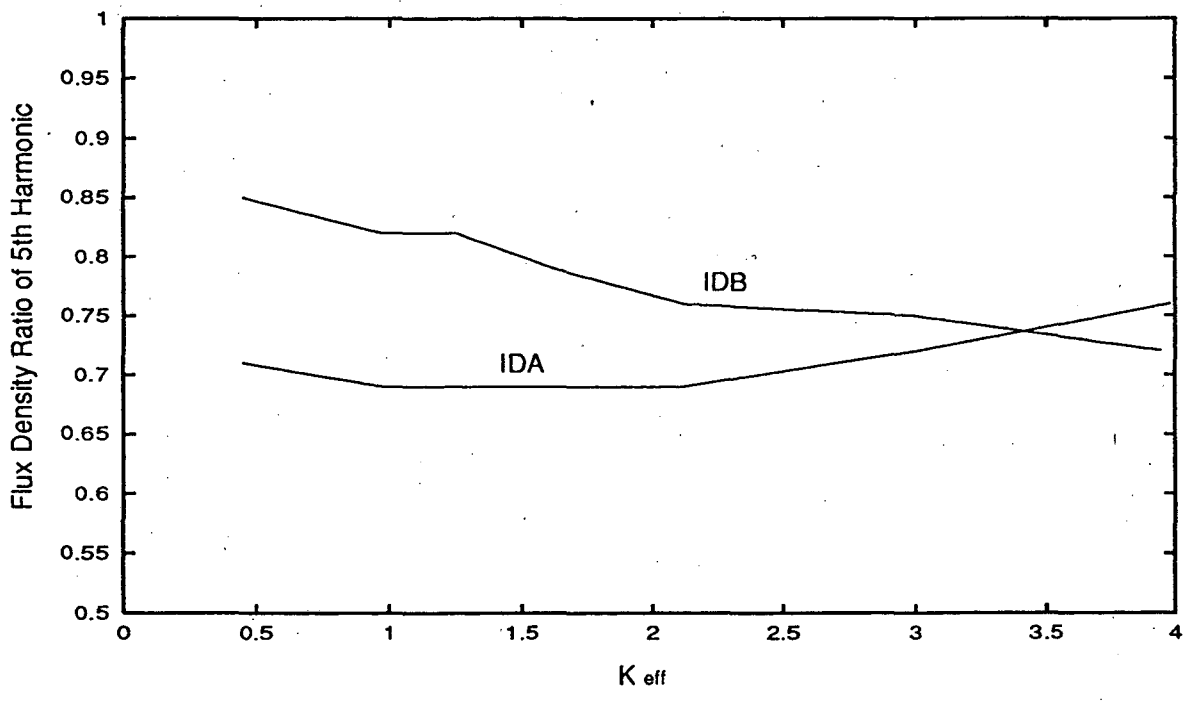

Figure 5. Calculated flux density ratio, real over ideal, as function of deflection parameter.

4. INTEGRAL FIELD DISTRIBUTION

In this section we will examine integrated field errors that potentially affect electron beam dynamics and lifetime. Figure 6 shows a plot of normal integrals, $I_y = \int B_y dz$, as a function of lateral position, x. The data is from measurements of IDB at 14 mm gap before any integral corrections were applied. Uncorrected integral data for IDA is similar. The total integral, I_t, is plotted along with I_u, I_d, and I_m, the components from the upstream end, the downstream end, and the middle (the portion of the device excluding the ends), respectively. Remember from the discussion in the introduction, the signature of the fields at the ends is fundamentally different than that in the middle since this represents a truncation of the periodic field. Note that the most of the integral error, or nonuniformity in integral value as a function of x, is due to the integral distribution in the middle of the device, and that the level of error is most significant outside the magnetic aperture of ±7 mm. The error within the magnetic aperture is mostly a gradient which is equivalent to an integrated normal quadrupole of about 280 G; this level is approximately double the specified tolerance. An integrated quadrupole in an insertion device represents a break in the symmetry of distributed focusing through the storage ring. The effect of errors outside the magnetic aperture is on beam dynamic aperture. Although a hard specification does not yet exist for the tolerable level, the uncorrected errors at extreme values of x are quite large and judged to be unacceptable.

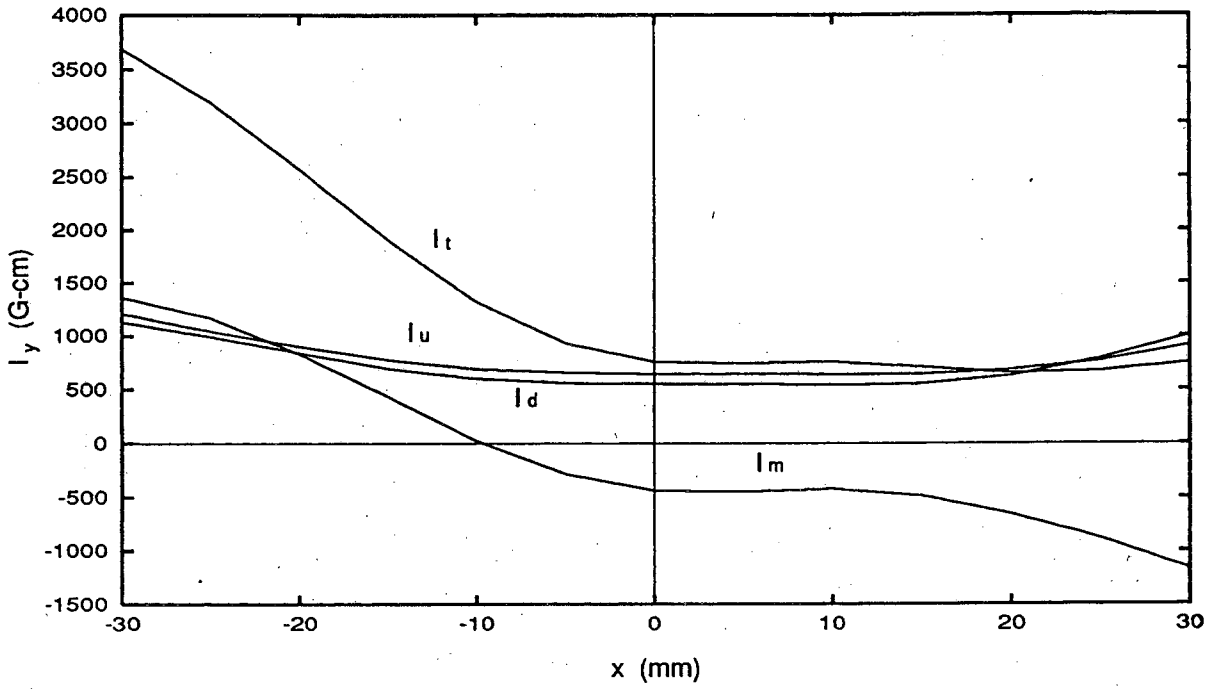

Figure 6. Uncorrected line integral measurements of B_y for IDB at 14 mm gap as a function of lateral position x. I_t is the total integral; I_u and I_d, are integrals from upstream and downstream ends, respectively; and I_m is the integral from the middle.

Figure 7 shows a graph of skew integrals, $I_x = \int B_x dz$. These data are from integral coil measurements and, therefore, only the total integral is measured. However, unlike B_y, B_x does not have a periodic structure (B_x is zero on the midplane of an ideal device), and, therefore, there is no structural differentiation between the ends and the middle. The distribution of I_x represents a significant gradient over the central region, which is equivalent to an integrated skew quadrupole of approximately 500 G within the magnetic aperture. This quantity is several times beyond the tolerable level. A skew quadrupole results in coupling of horizontal and vertical electron beam oscillations and can contribute to a growth in beam emittance, and thus a reduction in brightness. The largest errors are outside the magnetic aperture. These have

the same implications on dynamic aperture as do errors in I_y.

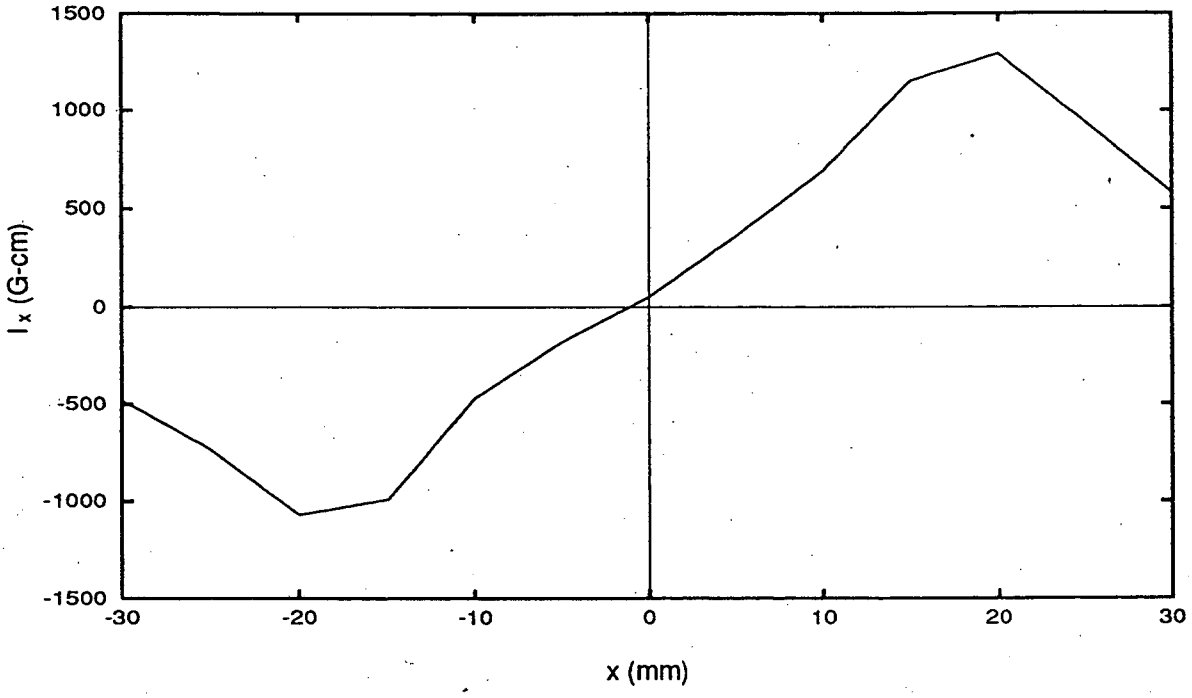

Figure 7. Uncorrected line integral measurements of B_x for IDB at 14 mm gap as a function of lateral position x.

A method for correcting normal and skew errors, both within the magnetic aperture and outside, has been devised by Hoyer[8], consisting of a lateral array of trim magnets. The principle of this device is to incorporate a field distribution at the ends that cancels the accumulated integral distribution in the middle of the device. The mechanism is illustrated in Figure 8. A cartridge is incorporated into the magnetic structure between the field clamp and the first pole. A total of four cartridges are installed, on top and bottom and at each end. Each cartridge contains up to nine separately adjustable individual permanent magnets, or "magic fingers." The permanent magnet fields are oriented vertically. The field distribution is adjusted by placing different sized magnets in the various locations and by adjusting the vertical displacement relative to the insertion device midplane. The multiple trim magnet (MTM) cartridge is designed so that the magic fingers can be easily adjusted.

The MTM can be used to change both the normal, or vertical, field and skew, or horizontal, field distributions. Normal fields are altered by maintaining normal symmetry; i.e., if a magnet is installed and adjusted in the bottom cartridge, the same magnet with the same polarity and adjustment must be installed in the top cartridge. Skew symmetry is maintained by installing magnets of opposite polarity in the top and bottom. Since the MTM is used to correct for both normal and skew errors, skew and normal corrections are combined at each end. In other words, the corrections have neither normal nor skew symmetry.

Figure 9 shows the integrated normal field distribution after correction. There are several points to note. First of all, the uniformity of I_t is significantly improved relative to the uncorrected fields of Figure 7. Second, the field distribution applied at the upstream and downstream ends is very nearly equal. Third, the integral distribution in the middle (not shown in Figure 9) is unchanged. And fourth, since I_t is measured as a line integral parallel to the axis, this quantity represents integral errors for particles following trajectories parallel to the axis. This is a good representation of errors that apply to the main electron beam, but not for those that apply to scattered particles, which do not necessarily follow trajectories parallel to the axis.

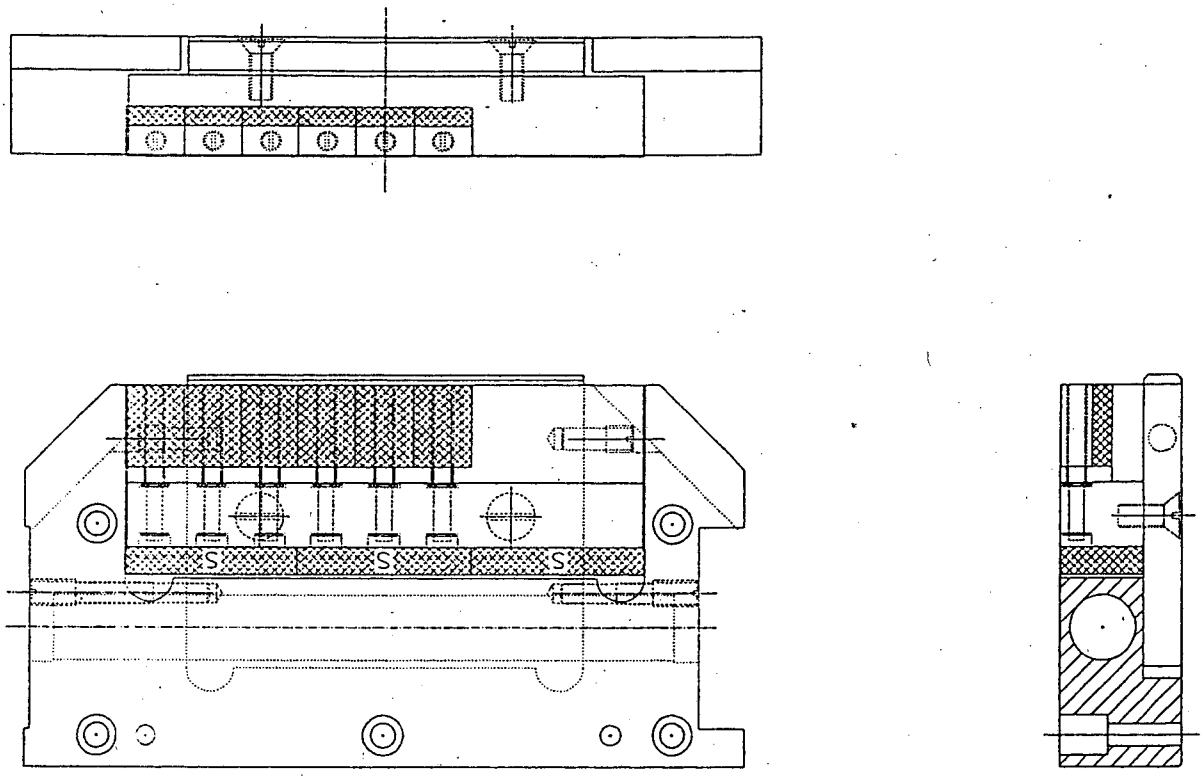

Figure 8. Multiple trim magnet cartridge design.

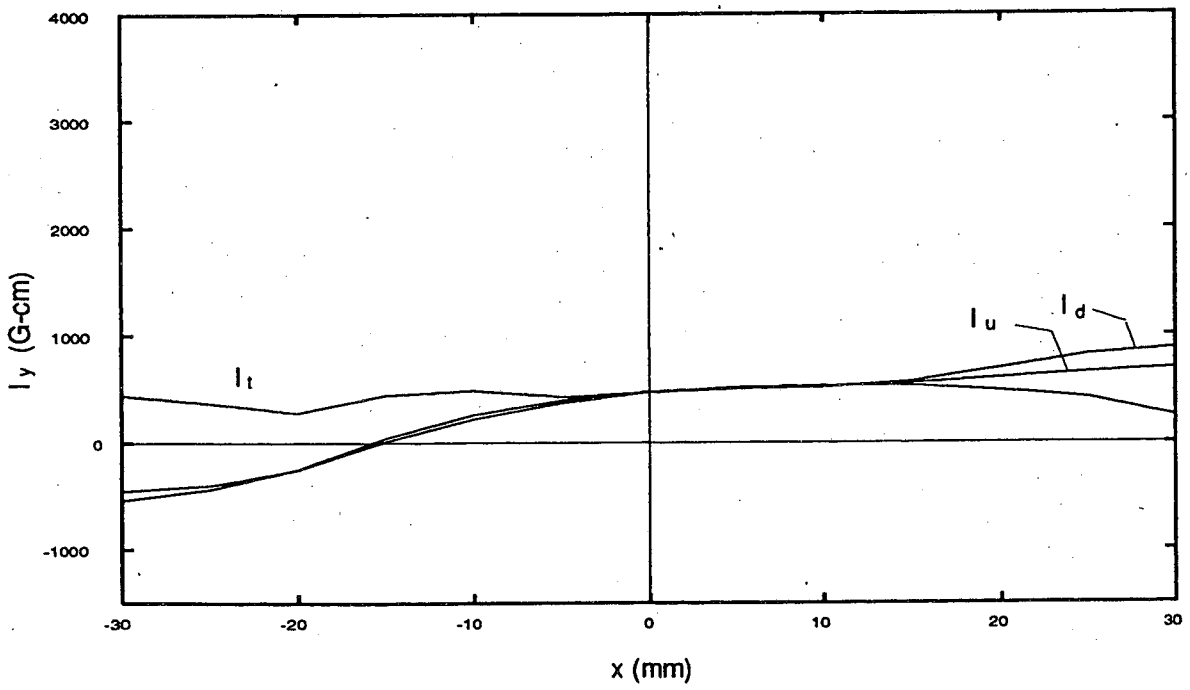

Figure 9. Line integral measurements of B_y for IDB at 14 mm gap after correction.

An arbitrary balance of corrections at both ends can be applied to correct for line integral errors parallel to the axis; in other words, it does not matter where along the line the correction is made. The same is not true for line integrals that follow other trajectories. A scheme that applies the required corrections according to the prescription illustrated in equation (7) below provides the best correction for arbitrary trajectories through the device.

$$\begin{aligned} \textit{downstream corrections} &= \frac{1}{2}(I_{mn} + I_{ms}) + I_{dn} + I_{ds} \\ \textit{upstream corrections} &= \frac{1}{2}(I_{mn} + I_{ms}) + I_{un} + I_{us} \end{aligned} \tag{7}$$

The symbols I_m, I_u, and I_d refer to integral errors corresponding to the middle, upstream end, and downstream end, respectively. The subscripts $_n$ and $_s$ refer to the normal and skew components, respectively. The correction applied at each end cancels all errors local to that end as well as half of the error corresponding to the middle of the device. The normal and skew error corrections are combined at each end. Notice that Figure 9 illustrates a correction that follows this prescription.

Figure 10 shows the integrated skew errors after correction. The error reduction is similar to that for the normal components.

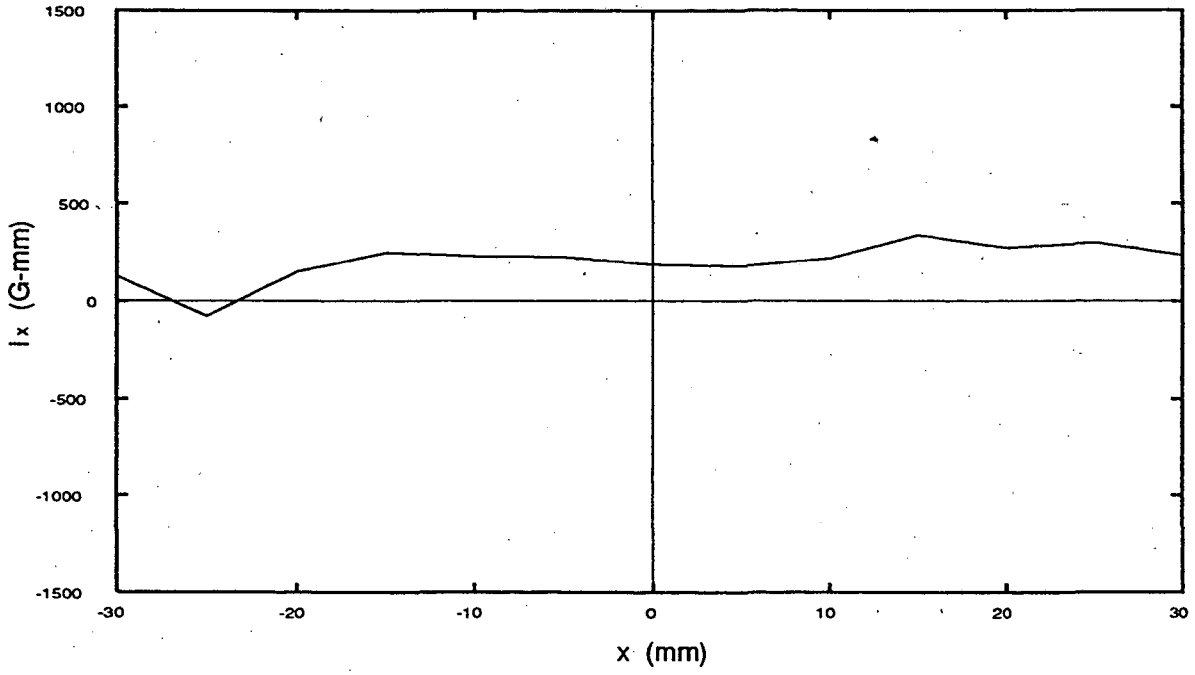

Figure 10. Line integral measurements of B_x for IDB at 14 mm gap after correction.

5. ACKNOWLEDGMENT

This work was supported by the Director, Office of Energy Research, Office of Basic Energy Science, Materials Science Division of the U. S. Department of Energy, under contract No. DE-AC03-76SF000098.

6. REFERENCES

1. K. Halbach, "Permanent magnet undulators", J. Phys. (Paris) 44, C1-211 (1983).
2. D. E. Humphries, J. Chin, R. Connors, J. Cummings, T. Keffler, W. Gath, E. H. Hoyer, B. M. Kincaid, P. Pipersky, "Precision alignment of the ALS U5 and U8 undulators," SPIE Proceedings Vol. 2013 (July 1993).
3. D. Humphries, K. Halbach, E. Hoyer, B. Kincaid, S. Marks, R. Schlueter, "Modeling and Measurement of the ALS Undulator End Magnetic Structures," IEEE PAC (May 1993).
4. S. Marks, C. Cork, E. Hoyer, D. Humphries, B. Kincaid, D. Plate, A. Robb, R. Schlueter, C. Wang, "Insertion Device Magnet Measurements for the Advanced Light Source:, IEEE PAC (May 1993).
5. B. Kincaid, "Random Errors in Undulators and Their Effects on the Radiation Spectrum," J. Opt. Soc. Am. B/Vol. 2, No. 8 (1985).
6. "U5.0 Undulator Conceptual Design Report," Lawrence Berkeley Laboroatory Report PUB-5256, (1989).
7. C. Wang, "Concise expression of a classical radiation spectrum," Phys. Rev. E, (June 1993).
8. E. Hoyer, "Multiple Trim Magnets," Lawrence Berkeley Laboratory Engineering Note, M7354.

LAWRENCE BERKELEY LABORATORY
UNIVERSITY OF CALIFORNIA
TECHNICAL INFORMATION DEPARTMENT
BERKELEY, CALIFORNIA 94720